JVI Journals.ASM.org

Natural Variation in the Heparan Sulfate Binding Domain of the Eastern Equine Encephalitis Virus E2 Glycoprotein Alters Interactions with Cell Surfaces and Virulence in Mice

Christina L. Gardner,[a] Jo Choi-Nurvitadhi,[a] Chengqun Sun,[a] Avraham Bayer,[b] Jozef Hritz,[c]* Kate D. Ryman,[a] William B. Klimstra[a]

Center for Vaccine Research and Department of Microbiology and Molecular Genetics,[a] Magee-Women's Research Institute,[b] and Department of Structural Biology,[c] University of Pittsburgh, Pittsburgh, Pennsylvania, USA

Recently, we compared amino acid sequences of the E2 glycoprotein of natural North American eastern equine encephalitis virus (NA-EEEV) isolates and demonstrated that naturally circulating viruses interact with heparan sulfate (HS) and that this interaction contributes to the extreme neurovirulence of EEEV (C. L. Gardner, G. D. Ebel, K. D. Ryman, and W. B. Klimstra, Proc. Natl. Acad. Sci. U. S. A., 108:16026–16031, 2011). In the current study, we have examined the contribution to HS binding of each of three lysine residues in the E2 71-to-77 region that comprise the primary HS binding site of wild-type (WT) NA-EEEV viruses. We also report that the original sequence comparison identified five virus isolates, each with one of three amino acid differences in the E2 71-to-77 region, including mutations in residues critical for HS binding by the WT virus. The natural variant viruses, which possessed either a mutation from lysine to glutamine at E2 71, a mutation from lysine to threonine at E2 71, or a mutation from threonine to lysine at E2 72, exhibited altered interactions with heparan sulfate and cell surfaces and altered virulence in a mouse model of EEEV disease. An electrostatic map of the EEEV E1/E2 heterotrimer based upon the recent Chikungunya virus crystal structure (J. E. Voss, M. C. Vaney, S. Duquerroy, C. Vonrhein, C. Girard-Blanc, E. Crublet, A. Thompson, G. Bricogne, and F. A. Rey, Nature, 468:709–712, 2010) showed the HS binding site to be at the apical surface of E2, with variants affecting the electrochemical nature of the binding site. Together, these results suggest that natural variation in the EEEV HS binding domain may arise during EEEV sylvatic cycles and that this variation may influence receptor interaction and the severity of EEEV disease.

The *Alphavirus* genus of the *Togaviridae* contains arthropod-borne viruses that can cause febrile illness, viral arthritis, and encephalitis. Among the encephalitis-causing viruses, North American strains of eastern equine encephalitis virus (NA-EEEV) are uniquely neurovirulent, resulting in mortality in 35 to 70% of symptomatic human cases and permanent neurological sequelae in a similar fraction of survivors (1). While typically, a small number of humans are symptomatically infected each year, the severity of EEEV disease and a recent increase in both human cases and detection of infected human-feeding mosquitoes (2, 3) have raised substantial concern, as there are no commercially licensed vaccines or antiviral therapeutics available to combat EEEV infection. Recently, we demonstrated that naturally circulating strains of NA-EEEV bind to heparan sulfate (HS) on cell surfaces and that this interaction promotes neurovirulence most likely through the following two mechanisms: (i) limiting virus replication in lymphoid tissues, leading to avoidance of innate immune and interferon responses to virus infection, and (ii) directly increasing virus infectivity for brain tissue (4). As of yet, no viral- or host-associated indicators of disease severity have been identified. However, a recent review of human pediatric cases concluded that more-extensive prodromal disease is correlated with survival (5).

Protein ligands typically bind HS through ionic interactions between sulfate groups on the HS chain and positively charged amino acids in the protein (6, 7). Consistent with a canonical mechanism of HS binding, we identified a putative HS binding domain for naturally circulating NA-EEEV involving three lysine residues in the E2 71-to-77 (71-77) region (4). Positively charged residues can also be selected in many viruses through routine cultured cell amplification procedures, and HS binding is a common phenotype of laboratory virus strains and live-attenuated vaccines (8–12). However, in contrast with EEEV, low-passage-number strains of most arthritogenic alphaviruses do not appear to bind HS efficiently; yet limited passage of these viruses *in vitro* can select for the phenotype (4, 9, 10, 13, 14) (C. L. Gardner, C. Sun, D. L. Vanlandingham, J. Hritz, T. Y. Song, M. B. Rogers, S. Higgs, W. B. Klimstra, and K. D. Ryman, unpublished data).

The ease with which such mutations accrue during *in vitro* amplification suggests that the HS binding phenotype may be variable even with naturally circulating viruses. We originally identified HS as an attachment receptor for naturally circulating NA-EEEV by comparing the translated E2 glycoprotein amino acid sequence of the prototypic NA-EEEV strain FL91-4679 to those of multiple minimally tissue culture-amplified isolates as well as 20 field isolates derived from tissues of infected crows, horses, and mosquitoes without *in vitro* amplification (15–17). Only 19 of the 61 total isolates and only one of the field samples exhibited any difference with FL91-4679 regardless of year, site of isolation, or whether the virus was derived from equines, avian species, or mosquitoes, reflecting a remarkable degree of conservation (4).

Here, we report that, while the overall amino acid sequence of the E2 glycoprotein of NA-EEEV strains is highly conserved, the

Received 5 April 2013 **Accepted** 21 May 2013
Published ahead of print 29 May 2013
Address correspondence to William B. Klimstra, Klimstra@pitt.edu.
* Present address: Jozef Hritz, EITEC, Masaryk University, Brno, Czech Republic.

doi:10.1128/JVI.00937-13

putative HS binding domain may represent a "hot spot" for amino acid sequence variation with significant consequence to virus biology. Of the 61 isolates aligned, five NA-EEEV isolates possessed a total of three differences in the putative HS binding domain, including changes in residues that we demonstrate are critical for efficient HS binding by the wild-type (WT) virus. Each natural variant had only one difference in the domain, but all of the differences altered the charge balance of the domain in comparison with the WT, either increasing or decreasing numbers of positively charged residues. When reconstituted in cDNA clones of WT NA-EEEV or an attenuated chimeric virus derived from NA- and South American (SA)-EEEV, each of the mutations altered HS dependence of infection and heparinase sensitivity by progeny viruses as well as type I interferon (alpha and beta interferon [IFN-α/β]) induction (a measure of prodromal disease) and virulence in mice. These results suggest that HS binding may vary in natural NA-EEEV isolates, that variants may elicit different degrees of prodromal disease, and that particular characteristics of HS binding are linked to the severity of encephalitic disease. To begin to understand the structure of HS binding sites in EEEV and correlate HS binding characteristics and virulence with domain structure and charge distribution, we have created an electrostatic homology model of the EEEV WT and variant virus heterodimeric E1/E2 spikes based upon the recent crystal structure of Chikungunya virus (CHIKV) E1/E2 (18). This model represents the first depiction of an HS binding domain confirmed to be utilized by a naturally circulating arbovirus. It is being used to determine the physicochemical basis of differential HS binding and facilitate prediction of mutations that confer HS binding but reduced neurovirulence for use in rational vaccine design.

MATERIALS AND METHODS

Ethical statement. All animal procedures were carried out in accordance with AAALAC-approved institutional guidelines for animal care and use and approved by IACUC.

EEEV sequence analyses. Nucleotide sequences of the E2 gene from 62 strains of NA-EEEV (15–17) were downloaded from the National Center for Biotechnology Information and translated into amino acid sequences starting with the amino-terminal amino acids of the mature E2 protein. Amino acid sequences were aligned using Vector NTI software (Invitrogen).

Viruses and replicons. The NA-EEEV FL93-939 and North American/South American BeAr436087/FL93-939 (NA/SA) chimeric virus cDNA clones (17) were gifts from Scott Weaver (UTMB). Construction of the HS binding-deficient 71-77 mutant full-length NA-EEEV virus, NA/SA chimeric virus, and replicon helper has been described (4, 17). T71, Q71, and K72 natural variant viruses (WT EEEV and NA/SA chimeras) and replicon glycoprotein helpers were created using the QuikChange II XL mutagenesis kit (Stratagene). Virus and replicon stocks were prepared and titers were determined on BHK-21 cells as described previously (13, 19). BHK-21 cell plaque sizes were measured on neutral red-stained monolayers. Infectious units in replicon stocks were determined via fluorescence microscopy (Olympus CKX41 microscope with the Endow green fluorescent protein [GFP] filter set) for GFP after BHK-21 cell infection as described previously (20). Virus-specific infectivities (PFU/microgram of protein) were determined as described previously (4).

Heparan sulfate interaction studies. Control CHOK1 cells and glycosaminoglycan (GAG)-deficient pgsA745 and heparan sulfate (HS)-deficient pgsD677 CHO cells were infected with equal dilutions of each virus or replicon, and infected cells were enumerated by plaque assay. For heparin competition, viruses were reacted with indicated concentrations of heparin or bovine serum albumin (BSA; Sigma) for 30 min on ice and then the preparations were used to infect BHK-21 cells for 30 min on ice, followed by washing with virus diluent (VD) (Opti-MEM growth medium; Invitrogen) prior to overlay, transfer to 37°C, and plaque assay. For infection in high-ionic-strength medium, viruses were diluted into RPMI-1% donor calf serum (DCS) buffer supplemented to the indicated NaCl concentration and cells were infected for 30 min at 37°C, followed by plaque assay. For heparinase assays, BHK monolayers were incubated with various concentrations of either heparinase I, heparinase II, or heparinase III at 37°C for 1 h, followed by washing with VD and infection with the indicated viruses. Overlay was applied 1 h after infection, and a standard plaque assay was performed.

Mouse infections and pathogenesis studies. Groups of five 8-week-old CD-1 mice (Charles River Laboratories) were infected either intracranially (i.c.) or subcutaneously (s.c.) in both rear footpads with 10 μl of each diluted virus or 10 μl of VD for mock infections. Virus inocula containing equal particle numbers were created by adjusting the dilution of titered virus/replicon stocks to reflect specific infectivity calculations for purified viruses such that equal virus protein concentrations were delivered. Virus- and mock-infected mice were observed at 24-h intervals until disease signs arose and every 12 h thereafter. At each time, mice were scored for signs of disease and weighed. Average survival times (AST) and percent mortality (mice that either died or were euthanized) were calculated as described previously (21). IFN-α/β in sera of infected mice was determined by biological assay as described previously (19).

Statistical analyses. Statistical significance for mortality curves was determined by a Mantel-Cox log-rank test (GraphPad Prism software), and for other experiments, Student's *t* test with two-sample equal variance (Microsoft Excel) was used. All experiments were conducted at least twice with similar results.

Electrostatic homology model. The homology model of the EEEV FL93-939 strain E1/E2 trimer and its mutants was constructed based on sequence alignment with the 05-115 CHIKV strain used recently to determine the E1/E2 spike crystal structure (Protein Data Bank [PDB] code 2XFB) (18) using Modeler version 9v8 (22). The models of the EEEV E1/E2 trimer included the E2 N-terminal tail that is missing in the CHIKV template trimer structure (PDB code 2XFB) (18). The presence of the N-terminal tail was found to have significant influence on the electrostatic potential in the areas of interest in the current studies (E2 amino acids [aa] 70 to 80). Consequently, in our representations of the EEEV heterodimers, there are some minor differences in the electrostatic potential between individual E2 monomers. This results from the fact that the template trimer structure (PDB code 2XFB) (18) did not exhibit complete C3 symmetry and the newly generated EEEV N-terminal tails lack the C3 symmetry because we did not apply symmetry restraints in the modeling. Having three different low-energy conformations of N-terminal tails gives an advantage by improved sampling and avoiding the possible incorrect interpretation of amino acid sequence variation effects on electrostatics that may be an artifact of one particular N-terminal tail conformation. Reflecting this approach, our model is suitable to determine the effects of amino acid sequence variation that are observed within all three monomeric units despite having different N-tail conformations. Charges of individual atoms and their radius parameters based on an amber force field (23) were generated by the pdb2pqr program (24). Electrostatic potential was generated by the Adaptive Poisson-Boltzmann Solver (APBS) package (25). A linearized Poisson-Boltzmann equation was applied with a dielectric constant of 2.0 for protein and 78.0 for solvent. Electrostatic potential on solvent-accessible surfaces in the range of −5 kT to 5 kT and with a solvent radius of 1.4 Å was visualized with the PyMol Molecular Graphics System (Schrodinger, LLC).

RESULTS

Mapping of lysine residues involved in HS-dependent infection by WT NA-EEEV. In our previous analysis, three lysine residues at the E2 glycoprotein positions 71, 74, and 77 were mutated to alanine, eliminating HS binding by the virus and defining the extent of the primary HS binding domain (4). We have now generated

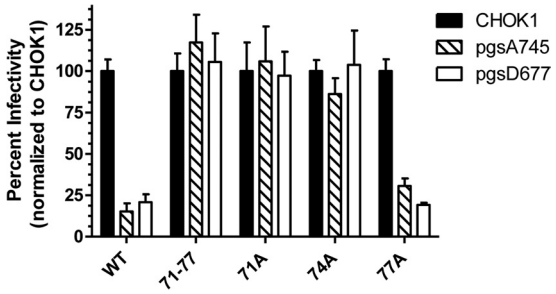

FIG 1 Dependence of infectivity of EEEV HS binding domain mutants upon GAGs or HS. Triplicate monolayers of control CHOK1 cells or GAG-deficient pgsA745 or HS-deficient pgsD677 cells were infected with each replicon for 1 h at 37°C. GFP-positive cells were then counted at 24 h postinfection. Data are presented as changes in titer in the absence of all GAGs or HS alone, normalized to titers on CHOK1 cells set to 100% infectivity. Error bars are standard deviations.

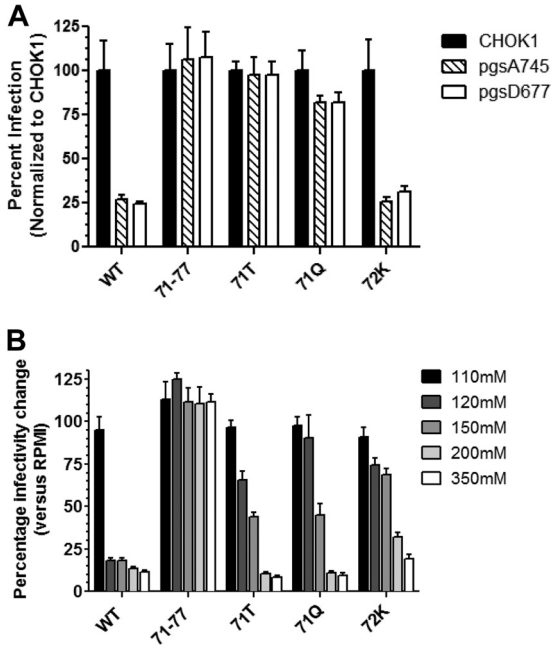

FIG 2 Dependence of infectivity of EEEV natural variants upon GAGs or HS or in buffer of increasing ionic strength. (A) Triplicate monolayers of control CHOK1 cells or GAG-deficient pgsA745 or HS-deficient pgsD677 cells were infected with each virus for 1 h at 37°C. Plaques were then counted at 48 h postinfection. Data are presented as changes in titer in the absence of all GAGs or HS alone, normalized to titers on CHOK1 cells set to 100% infectivity. (B) Viruses were diluted into RPMI buffer supplemented with NaCl to achieve each desired concentration and used to infect triplicate BHK cell monolayers for 1 h at 37°C. Cells were then overlaid, and plaques were counted at 24 hpi. Data are presented as the alterations in infectivity at each NaCl concentration, normalized to RPMI alone set to 100% infectivity (data not shown). Error bars are standard deviations.

enhanced green fluorescent protein (eGFP)-expressing replicons (as described in reference 4) with each lysine individually mutated to alanine to determine the contribution of each lysine to dependence of infection upon HS. Comparison of infectivities between CHOK1 and GAG- or HS-negative (pgsA745 or pgsD677) cells indicated that neutralization of individual positive charges at the 71 or 74 position resulted in an HS-independent infection phenotype (71, *P* value of >0.05 comparing infectivity on pgsA745 or pgsD677 cells with that on WT CHOK1; 74, *P* value of >0.05 comparing infectivity on pgsA745 with that on the WT and *P* value of <0.05 comparing infectivity on pgsD677 cells with that on the WT) similar to that of the combined neutralization of all three lysines, while neutralization of the lysine at position 77 had little effect (*P* value of >0.05 comparing infectivity on pgsA745 or pgsD677 cells with that on WT CHOK1 cells) (Fig. 1). This suggests that the HS binding site of WT EEEV is composed primarily of the position 71 and 74 lysines and that these residues cooperate in HS binding such that neutralization of either charge dramatically reduces infection of HS- or GAG-negative cells.

Effects of natural variation in the E2 HS binding domain upon HS binding by EEEV. The three natural variants identified in sequence comparisons were spread among five isolates (4) (Table 1), which may exhibit some temporal association; however, there is no apparent geographical association or single host (e.g., human, mosquito, equine, avian) associated with mutations shared by more than one virus (15–17). Notably, the E2 71T variation resulted in creation of an NXT (N = asparagine, X = any amino acid, T = threonine) N-linked carbohydrate addition site (Table 1). The E2 protein of this virus exhibited slowed migration versus all other EEEV strains when infected BHK cell lysates were separated on SDS-PAGE gels and stained with anti-EEEV antiserum, strongly suggesting that the site was modified in mammalian cells (DNS).

We used a series of cell interaction assays to evaluate the dependence of the variant viruses' infectivity upon HS compared to that of the WT and the 71-77 HS-negative mutant (Fig. 2 and 3).

TABLE 1 Amino acid sequence of the E2 HS binding domain and specific infectivity and plaque sizes of viruses used in this study

Virus	E2 69–77 amino acid sequence	Isolate[a]	Specific infectivity[b] (PFU/μg)	Plaque size[c] (mm)
WT	NGKTQKSIK	FL91-4679 and 42 others	1.0 ± 0.0	6.41 ± 0.44
E2 71-77A	NGATQASIA	Mutant	9.2 ± 1.4	4.24 ± 0.54
E2 71A	NGATQKSIK	Mutant	ND	ND
E2 74A	NGKTQASIK	Mutant	ND	ND
E2 77A	NGKTQKSIA	Mutant	ND	ND
E2 71Q	NGQTQKSIK	MA38, LA50	1.0 ± 0.4	3.81 ± 0.42
E2 71T	NGTTQKSIK	CT90, MS83	10.0 ± 1.4	4.00 ± 0.43
E2 72K	NGKKQKSIK	TX95	1.1 ± 0.2	1.87 ± 0.37

[a] Letters represent the state where the virus was isolated; the numbers immediately after the state abbreviation represent the year of isolation (15–17).
[b] Represented as fold reduction in specific infectivity versus that of the WT. ND, not done.
[c] ND, not done.

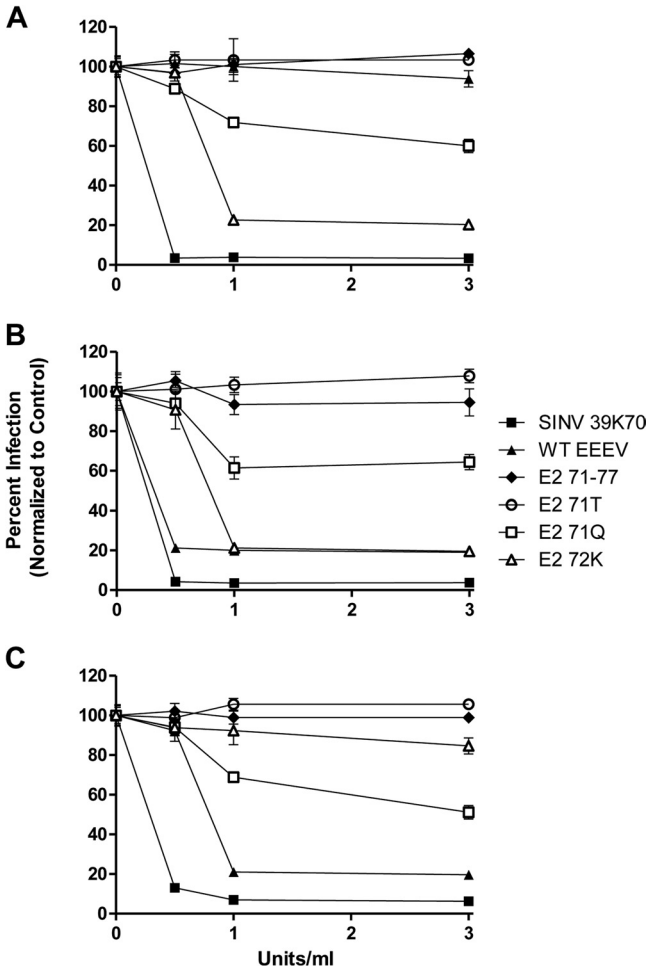

FIG 3 Sensitivity of infection by natural variants to heparinase digestion. BHK cell monolayers were washed with VD and then digested with either heparinase I (A), heparinase II (B), or heparinase III (C) for 1 h at 37°C and washed 2 times with VD prior to infection with the indicated viruses. At 48 h postinfection, plaques on the monolayers were enumerated. Data are presented as changes in infectivity with increasing heparinase concentrations, normalized to a no-heparinase control set to 100% infectivity. Error bars are standard deviations, and some are too small to be seen.

In infectivity measurement assays using GAG-negative pgsA745 or HS-negative pgsD677 CHO cells, the 71T variant exhibited no significant dependence upon GAGs in general or HS specifically for infection similar to that of the 71-77 mutant while the 71Q variant exhibited intermediate dependence and 72K was similar to the WT virus (Fig. 2A). Differences in infectivity between pgsA745 and pgsD677 cells were small for all viruses (Fig. 2A), indicating that infectivity enhancements due to GAG binding primarily reflected interaction with HS. BHK cell-specific infectivity measurements (infectious units/μg protein) were consistent in that viruses with no significant reduction in infectivity in the absence of HS (71-77 mutant and 71T) were not significantly different from each other ($P > 0.2$) and viruses either partially (71Q) or highly (WT, 72K) dependent upon HS for infection exhibited ~10-fold-higher specific infectivity and were not significantly different from each other ($P > 0.2$) (Table 1). We previously demonstrated with Sindbis virus (SINV) (13, 26, 27) that binding to HS increases association of virus particles with cells *in vitro* and, consequently, infection efficiency. BHK cell plaque sizes were also variable between viruses, with the most-HS-dependent viruses producing the largest (WT) and smallest (72K) plaques on BHK cells, respectively, and HS-independent (71-77, 71T) or partially dependent (71Q) viruses producing intermediate-sized plaques (Table 1). Competition of BHK cell infectivity with soluble heparin, a small, highly charged mimic of HS (6), generally followed these results (DNS), although the 71T virus was partially competed compared with 71-77, which demonstrated no competition. This may suggest that heparin has greater affinity for virus particles than HS and obscures other receptor binding sites possibly involving ionic interactions between particles and cells.

To examine the role of ionic interactions in HS binding and infectivity of EEEV viruses, we infected BHK cells in the presence of increasing concentrations of NaCl, from the RPMI control, which is ~103 mM NaCl, to RPMI supplemented to 350 mM NaCl (Fig. 2B). Increasing ionic strength can give an indication of HS binding affinity, as stronger HS interactions require higher ionic strength to disrupt (6, 8, 27). Consistent with minimal dependence upon HS, infectivity of the 71-77 mutant was resistant to all NaCl concentrations. In contrast, the HS binding WT virus was reduced ~80% in infectivity by concentrations above 110 mM. The 72K virus demonstrated higher resistance than the WT to all NaCl concentrations except 350 mM, possibly reflecting a stronger interaction with HS. Interestingly, the partially HS-dependent 71Q and HS-independent 71T viruses showed similar sensitivity profiles and were reduced at 200 mM and 350 mM similarly to the WT virus. Considering the lack of HS dependence of infection by 71T and the intermediate dependence of 71Q (Fig. 2A), this result may reflect an ionic interaction with cell surfaces separate from HS binding associated with the presence of either the additional carbohydrate modification in 71T or the lysine residues at E2 positions 74 and 77 in both viruses.

Finally, we examined the infectivity of each virus for BHK cells digested with the microbial heparinases heparinase I (Hep I), heparinase II (Hep II), and heparinase III (Hep III), which degrade cell surface HS (recently reviewed in reference 28). Hep II has the widest specificity for HS substrates, cleaving both HS and heparin with various sulfation patterns, while Hep I cleaves primarily highly sulfated heparin and Hep III cleaves primarily less-sulfated regions of HS (29, 30). Hence, the residual HS structure after digestion of cells differs between the lyases, and it is likely that viruses that maintain control levels of infectivity after digestion either do not interact with HS during infection or are capable of binding these residual HS structures (13). As expected, viruses with little infectivity dependence upon HS (71-77, 71T) were resistant to treatment of cells with all three of the heparinases (Fig. 3A to C). The 71Q virus, which exhibited intermediate infectivity dependence, showed a partial reduction with all three enzymes (Fig. 3A to C). Interestingly, the two highly HS-dependent EEEV viruses showed marked differences in sensitivity. The WT virus was highly sensitive to Hep III digestion but resistant to Hep I, while the converse was found with 72K (Fig. 3A and C). These viruses were similarly sensitive to Hep II but at slightly different concentrations (Fig. 3B). In contrast, the HS-binding but adult mouse-avirulent 39K70 SINV, included here as an HS binding control, was highly sensitive to all three heparinases. Together, these data suggest that incorporating a posttranslational carbohydrate modification or altering the positive charge balance in the E2 HS binding domain by point mutation can alter the degree and

nature of dependence upon HS for infectivity. Most importantly, NaCl infection and heparinase digestion assays suggest that single site mutations can change either the affinity of interaction or the HS structure to which viruses bind.

Effects of natural variation in the E2 HS binding domain upon virus-host interactions. Previously, we demonstrated that HS binding by the WT virus enhanced neurovirulence *in vivo* versus the 71-77 non-HS-binding mutant by increasing infectivity for cells in the central nervous system (CNS) and diminishing infection of lymphoid tissues and consequent induction of IFN-α/β in serum. Furthermore, a chimeric virus attenuated by incorporation of nonvirulent SA-EEEV strain BeAr436087 nonstructural proteins (nsPs) but expressing WT NA-EEEV structural proteins (SA/NA) caused 100% mortality when injected intracranially while the 71-77 mutant caused no mortality, implying an association between HS binding and EEEV neurovirulence (4). To determine if such an association existed with the natural variants and examine the phenotypes of the natural variants in animals, we infected adult CD-1 mice with either native viruses, differing only by the amino acids of the E2 HS binding site, or SA/NA chimeric viruses containing the SA BeAr436087 nsPs fused to structural proteins, differing only in the E2 HS binding sequence.

After s.c. infection with particle doses of each virus normalized, as described in Materials and Methods, to either 250 PFU or 10 PFU of the WT, as expected (4), the WT and 71-77, along with 71T and 71Q, caused 100% mortality at the 250-PFU dose, but at 10 PFU, only 71-77, 71T, and 71Q caused 100% mortality, with mice succumbing to infection between 6 and 7 days postinfection (p.i.) with either dose (Fig. 4A and B). However, 72K caused only 60% mortality ($P < 0.05$) at this dose, and both WT and 72K viruses caused less than 100% mortality at the 10-PFU dose, with the 72K virus completely avirulent ($P < 0.05$) (Fig. 4B). At 250 PFU, WT, 71T, and 71Q had similar survival times ($P > 0.05$) and 71-77 and 72K had significantly extended survival times ($P < 0.05$), while at 10 PFU, WT, 71-77, 71Q, and 71T had similar survival times ($P > 0.05$). Upon i.c. challenge of the 10-PFU animals with 1,000 PFU of WT EEEV 10 days after primary infection, none of the 72K-infected mice survived while all of the WT-infected mice survived, suggesting that the 72K virus did not establish infection at this dose. IFN-α/β induction in serum after s.c. infection at a lethal dose for all viruses (250 PFU) generally mirrored the HS binding phenotypes, as the HS-independent viruses 71-77 and 71T were significantly higher than WT or 72K (P values of <0.035 and <0.045, respectively) (Fig. 4C). The partially HS-dependent 71Q virus was not significantly different from either group ($P > 0.05$). Together, these results suggest that initiation of infection and/or spread after infection may be suppressed for viruses that bind HS efficiently and that there is an association between HS binding and suppression of IFN-α/β induction in serum when the natural route of infection is mimicked.

When mice were inoculated i.c. with 10 PFU, all viruses caused 100% mortality (Fig. 5A). However, shorter survival times generally correlated with the capacity to bind HS, as WT, 72K, and 71Q viruses were not significantly different from each other ($P > 0.05$) and were significantly shorter than 71-77 ($P < 0.02$). The non-HS-binding 71T was significantly different from WT and 71Q ($P < 0.05$) but not from 72K ($P > 0.05$), although the AST was longer (3.1 days versus 2.3 days, respectively). Results for a 250-PFU dose were similar (DNS). Inoculation of mice with 1,000 PFU of the SA/NA-EEEV chimeric viruses again segregated viruses by

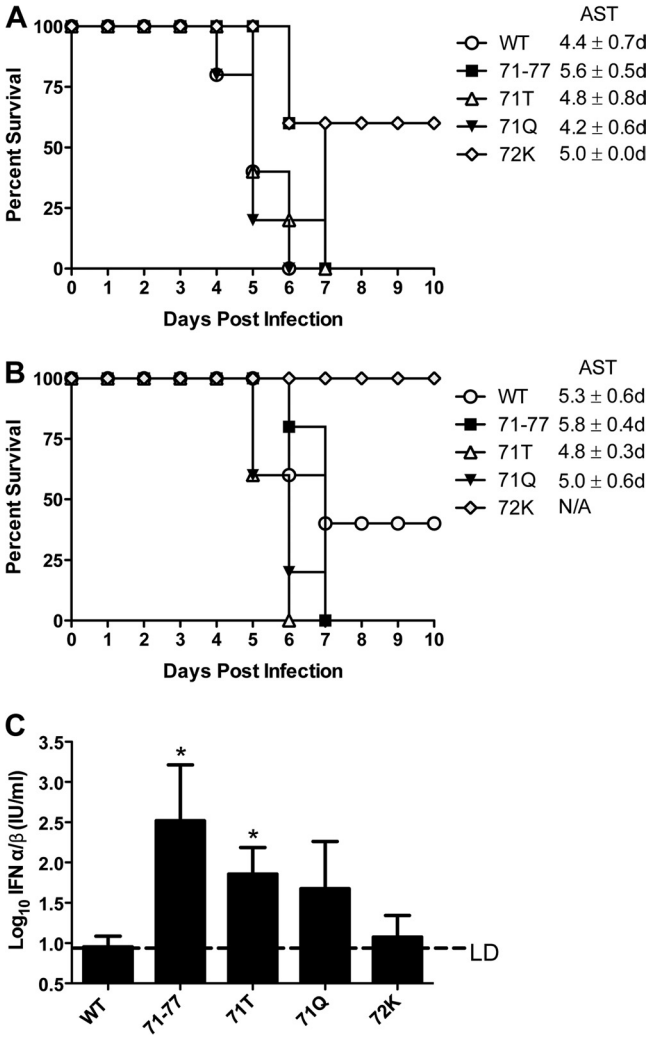

FIG 4 Effects of natural variation in E2 upon EEEV virulence in mice infected by a mimic of a natural route and subsequent induction of serum IFN-α/β. (A) Groups of five adult CD-1 mice were infected with each virus subcutaneously with a viral protein dose equivalent to either 250 PFU (A) or 10 PFU (B) of the WT EEEV. Mice either succumbing to infection or reaching euthanasia criteria were enumerated each day. Average survival times (AST) were calculated as described in Materials and Methods. (C) Measurement of serum IFN-α/β induction by bioassay at 48 h postinfection with 250-PFU equivalents of each virus as described in panel A. This was the time of maximal induction by the 71-77 virus in previous experiments (4). *, significantly different ($P < 0.05$) from WT and 72K; LD, limit of detection of the bioassay; N/A, not applicable; d, days. Error bars are standard deviations.

HS binding phenotype, as WT and 72K viruses caused 100% mortality, the 71Q virus caused 60% mortality, and the 71-77 and 71T viruses were avirulent (phenotypes reported previously for WT and 71-77 [4]) (Fig. 5B). Therefore, if viruses are delivered directly to the CNS without the viremia requirement to spread the virus to the CNS, the degree of infection dependence upon HS binding as measured in Fig. 2A is positively associated with virulence.

Structural mapping of the NA-EEEV HS binding domain. Based upon the crystal structure for the CHIKV E1/E2 heterodimer (18), the surface representation of electrostatic potential calculated by APBS (25) for the WT EEEV virus E2 protein in a trimer of E1/E2 heterodimers is shown (Fig. 6A and B). E1 is

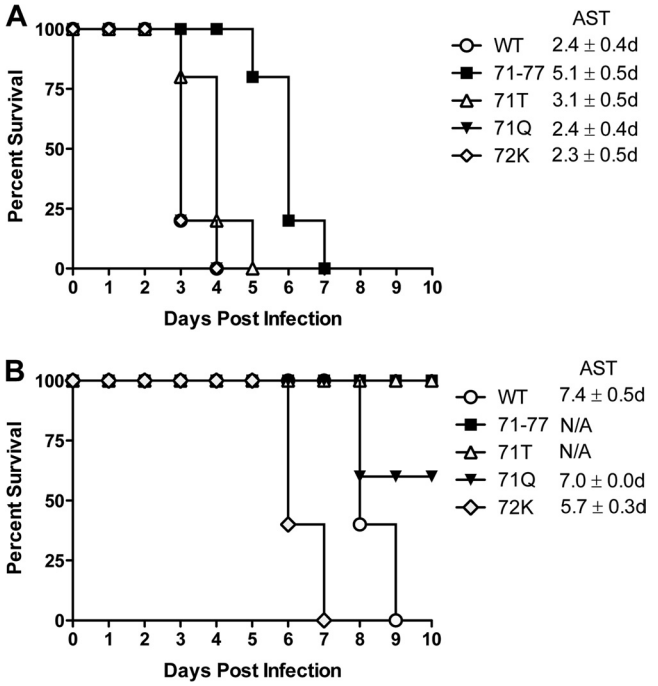

FIG 5 Effects of natural variation in E2 upon EEEV virulence in mice after direct infection of the brain. Groups of five adult CD-1 mice were infected with each virus intracranially with a viral protein dose equivalent to 10 PFU of the WT EEEV (A) or were infected with a viral protein dose equivalent to 1,000 PFU, with the NA/SA chimeric viruses differing only by the indicated residues in E2 (B). Mice either succumbing to infection or reaching euthanasia criteria were enumerated each day. Average survival times (AST) were calculated as described in Materials and Methods.

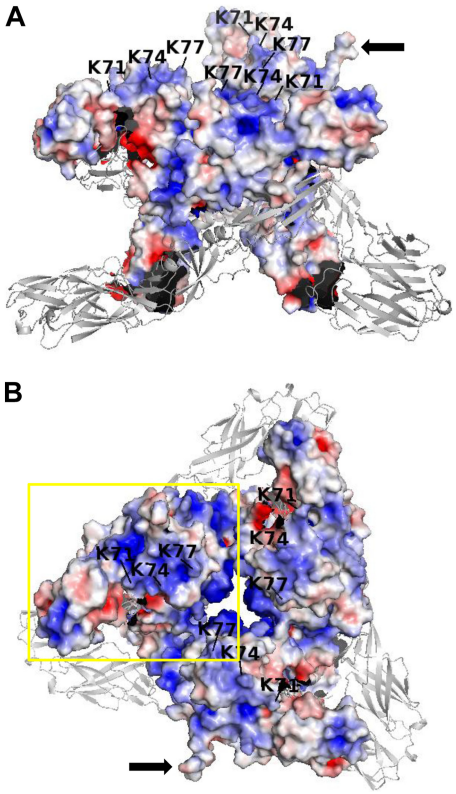

FIG 6 Three-dimensional electrostatic surface model of WT EEEV E1/E2 heterodimers in a mature spike complex. The EEEV electrostatic surface model was calculated based upon the CHIKV crystal structure (18) as described in Materials and Methods, with the E1 glycoprotein represented as a ribbon diagram and ambiguous interface regions between E1 and E2 in black. The lysine residues at positions 71, 74, and 77 in the E2 protein are indicated by black letters/numbers and black bars pointing to the specific residue. (A) Side view of the mature glycoprotein complex. (B) Top view of the complex. Black arrows point to the nonconstrained placement of the N terminus of E2 in a subset of heterodimers. The yellow box corresponds to the portion of a single heterodimer magnified in Fig. 7.

represented as a ribbon diagram, and ambiguous contact regions between E1 and E2 are shown in black. The disordered E2 amino-terminal tail (18) is shown but not constrained such that conformation varies between the three heterodimers.

The HS binding domain of E2 associated with position 71, 74, and 77 lysines is located near the inner apical surface of the E2 Ig-like domain A in the i5-i6 "wing" insertion region (as defined in reference 18) (Fig. 6A and B). Positively charged residues in this region, accumulated during cell culture adaptation, can play a role in HS binding by SINV (E2 70 Lys) (26), Venezuelan equine encephalitis virus (VEEV) (E2 76 Lys) (9), and CHIKV (E2 79 Lys, 82 Arg) (Gardner, unpublished data), with the SINV K70 essentially conferring efficient HS binding to the otherwise non-HS-binding TR339 strain (27). Mutation of all three of the 71, 74, and 77 lysines to alanine neutralized the charge all along this edge and is associated with HS-independent infection (Fig. 7A and B) (4). Data for HS dependence of infection indicate that with NA-EEEV, E2 71K and 74K are critical and cooperative mediators of HS interaction, but E2 77K appears to be minimally involved (Fig. 1 and 7C to E). Consistently, all of the natural mutants identified affect either the E2 71K or the adjacent E2 72 residue. Together, the 71 and 74 lysines create a positively charged site of about 22 Å by 15 Å toward the upper edge of the cleft between domains A and B into which the E1 fusion loop penetrates (Fig. 6E) (18). Importantly, this size is consistent with that of other charge models of HS binding sites (e.g., see references 31–33).

With respect to the natural variants, the effect of the 71Q variant appears similar to that of mutated alanine (Fig. 7C and F), reducing positive charge at the domain B-proximal leading edge of the domain A-domain B cleft. However, the effect of a polar residue at this position may be different from that of an uncharged residue (see Discussion). The 72K variant produces an additional eminence in the site and increases the positive charge density within the binding site (Fig. 7A and H). The effect of the presence of a carbohydrate modification in 71T cannot be shown in this model since it is not present in the CHIKV crystal (Fig. 7G) (18), and usually carbohydrates are flexible. However, since this variation has a larger inhibitory effect on HS interaction than 71Q, we infer that it acts by a combination of charge neutralization at E2 71 and steric hindrance by the carbohydrate moiety.

DISCUSSION

Effects of mutations to the 71-77 region of EEEV E2 upon HS binding and animal virulence. These studies represent the first description of natural variants in a confirmed HS binding site used by circulating arboviruses and the first localization of such a site in the three-dimensional structure of the alphavirus E1/E2 heterodimer. In addition, we demonstrate that the variations in the

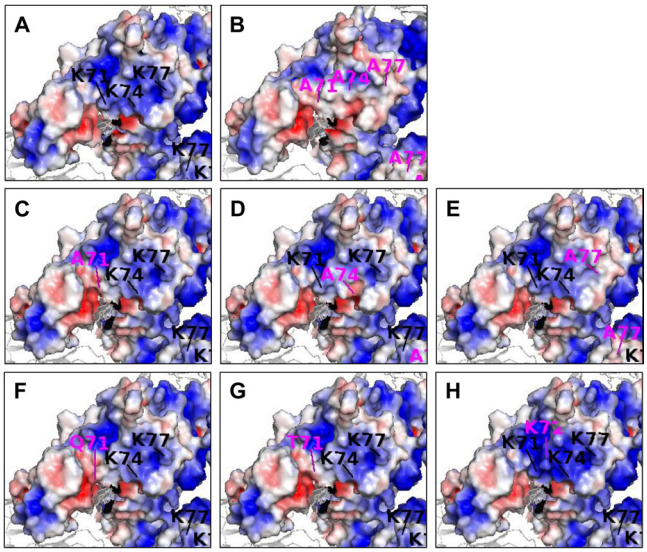

FIG 7 Magnified view of the effects of mutations or natural variations in the EEEV E1/E2 spike complex upon surface charge distribution. In addition to the WT (A), complete E1/E2 spike complex models were created for the 71-77 mutant (B), each mutant in which an amino acid was individually mutated to alanine, 71A, 74A, and 77A (C, D, and E, respectively), and the natural variants 71T (F), 71Q (G), and 72K (H), as in Fig. 6B, and the portion of the E1/E2 complex boxed in yellow was magnified approximately 2-fold. Mutant or variant amino acid substitutions are indicated with magenta letters/numbers, and bars and WT residues are indicated as in Fig. 6.

binding site alter HS interaction characteristics and virulence in an animal model of EEEV disease. Specifically, lower neurovirulence and greater IFN-α/β induction were associated with altered HS binding compared with WT EEEV, suggesting a possible mechanism for differing prodromal disease in humans. The sequence comparison data suggest that such mutations may be only rarely seen in NA-EEEV isolates (5 of 61 isolates [4]). While the possibility remains that these differences in the HS binding domain of NA-EEEV reflect *in vitro* adaptations arising during amplification of isolates, we have never observed mutation away from the HS binding phenotype during routine *in vitro* passage of alphaviruses.

To map the critical residues involved in HS binding by WT NA-EEEV, we initially mutated each of the three lysines in the 71-77 region individually to alanine and examined infection dependence upon all GAGs and HS specifically (4). The data suggest that HS is the primary GAG bound by WT EEEV and that the lysines at 71 and 74 are the critical residues for HS binding and they display cooperativity. Assuming that HS binding occurs through direct contacts with 71K and 74K, the positively charged area surrounding these two residues in the E2 domain A wing region may comprise the entirety of the HS binding site in WT NA-EEEV (Figure 7E). However, the participation of adjacent and possibly distant positively charged or polar residues cannot be ruled out. The location and structure of this natural binding site are possibly similar to those of sites acquired through cell culture adaptation with other alphaviruses that possess positively charged substitutions near E2 position 70 (9, 26) (Gardner, unpublished data). However, alphavirus HS binding sites acquired through cell culture adaptation can also map to the apical surface of E2 domain B (18, 34).

The comparison of the WT virus and the 71-77 HS-negative mutant, which has all three lysines mutated to alanine, demonstrated that each of the natural variants altered HS interactions *in vitro* and aspects of disease in animals. The 71T variant exhibited essentially HS- and GAG-independent infection of CHO cells, but the NaCl infection disruption and heparin competition assay suggested an HS-independent ionic component to infectivity. Since it appears by gel migration that the new carbohydrate addition site is modified in cells used for virus production, the bulk of the added moiety may either hinder the HS binding site sterically or alter conformation regionally to disrupt it and may also possibly participate in an ionic interaction with another receptor. The 71Q variant demonstrated partially HS-dependent infection, an intermediate ionic contribution to infectivity, and similar sensitivity to all heparinases. This may reflect a reduction in positive charge in the binding domain and through substitution of a polar residue. It is possible that 71Q and 71T differ primarily by the presence/absence of the carbohydrate modification. In contrast, the 72K virus showed an overall dependence upon HS for infection and particle infectivity similar to those of the WT, but the characteristics of the interaction with cell surfaces (optimum concentration for NaCl infection blocking, plaque size, heparinase sensitivity) suggested either an altered affinity for HS or binding to a different HS structure. This is not without precedent for viruses, as it has been proposed that different herpes simplex virus types and individual attachment proteins interact with different HS structures (reviewed in reference 35).

In comparison with the WT, differential interaction of viruses with HS measured *in vitro* was apparent for at least one of the variants in each animal experiment. At lower s.c. doses, the viruses that bound HS most efficiently (WT and 72K) were less able to either spread or establish infection *in vivo*, with 72K essentially failing to establish infection at the 10-PFU dose. However, when expressed in the attenuated background of the SA/NA chimeras and delivered to the brain, these viruses were highly virulent, with the 72K showing shorter AST than the WT, and confirmed the positive association of HS binding with neurovirulence and possibly the particular structure bound or binding affinity. In addition, the dependence of infection upon HS was correlated with suppression of IFN-α/β secretion into serum, with 71-77 and 71T inducing the most, WT and 72K inducing the least, and 71Q intermediate, although the values for this virus were not statistically significant from either group.

It is worth noting that a positively charged lysine residue at the 70 position of SINV E2 acquired during cell culture adaptation of the virus can act with a histidine at E2 55 to alter HS interaction (and subsequent infection features [1]) and confer adult mouse neurovirulence to SINV (27, 36). In the heparinase assays, the SINV with 70K only was highly sensitive to all three heparinases. However, EEEV viruses whose E2 proteins conferred adult virulence to the NA/SA chimeras (WT, 72K) exhibited differential heparinase sensitivity. It is tempting to speculate that the NA-EEEV E2 may already possess a function similar to that provided by E2 H55 in SINV, although there is no obvious sequence similarity in this region. Further, it is possible that differential heparinase sensitivity is associated in some manner with neurovirulence.

Structural characteristics of the EEEV HS binding site. Recently, a cationic-polar-cationic direct HS interaction (CPC) motif was identified by comparison of three-dimensional binding site structures of multiple HS binding proteins (37). The authors sug-

gested that the polar residues might promote discrimination between binding of different HS structures, with glutamine preferred for 2-*O*-sulfo-α-L-iduronic acid binding and asparagine preferred for N,O6-disulfo-glucosamine binding and the polar amino acids threonine, serine, and tyrosine contributing to a lesser extent. Our structural mapping of the position of the 71-77 region and the location of two polar residues between the critical 71K and 74K is consistent with this idea. It is possible that, naturally, the tyrosine at 72 and glutamine residue at position 73 contribute to this motif. This may suggest that the K72 lysine in TX95 increases/alters HS interaction by increasing the positive charge in the binding site and by removing a polar amino acid. Similarly, the 71Q mutation eliminates a positively charged residue but adds a polar residue. This is consistent with the fact that each of these mutations alters sensitivity to Hep I and Hep III in different manners compared with the WT, supporting the idea that the three different viruses bind different HS structures. We are currently using computational modeling to fit HS structures into the WT and natural variant EEEV binding sites to further elucidate the underpinnings of differential HS binding. It should be noted that our model does not consider conformational changes that might occur upon HS interaction and that have been demonstrated during initial virus-cell contact (38). These may have functional implications considering the close proximity of the E1 fusion loop and the proposal that its initial movement may occur prior to low pH exposure (18).

Role of HS binding in the EEEV natural replication/transmission cycle. While it seems clear that the HS binding is a characteristic of dominant virus genotypes within naturally circulating NA-EEEV populations, the role of this phenotype is not obvious. Our data (this study and those in references 4 and 20) suggest that HS binding, along with the inability of NA-EEEV to initiate translation in myeloid cells, greatly suppresses the innate immune response of infected vertebrates, providing an understandable selective advantage. This phenotype concomitantly increases brain replication and neurovirulence. However, HS binding also suppresses the rate of virus dissemination and the duration and magnitude of viremia (4, 9, 39). Intuitively, suppression of the innate immune response and viremia should have opposing impacts upon viral fitness in vertebrates and transmission between vertebrates and mosquito vectors.

As described above, the 72K virus initiates infection of mice from the natural route more poorly than the WT, which is also less likely to initiate a systemic infection than intermediately binding (71Q) or non-HS-binding (71-77, 71T) viruses. Historically, the strict ornithophilic feeding characteristics of the principal enzootic EEEV vector, *Culiseta melanura*, have been suggested to account for the limited instances of human infection (e.g., see references 40 and 41). However, the virus has increasingly been found in human-feeding species, such as *Aedes albopictus* (3) and *Coquillettidia perturbans* (2, 42), yet the human case rate remains low. We propose that efficient HS binding may also contribute to this phenotype. It is, perhaps, fortunate that the extreme neurovirulence of EEEV may be linked to a phenotype that may also limit its spread to and within mammalian hosts. Additional human serosurveys in states such as Massachusetts, where human-feeding mosquitoes are infected (42), may shed light on this issue.

Finally, the mouse model used in the current studies is a mammalian disease model, which is unlikely to provide the complete ensemble of selection pressures present during cycling of EEEV between mosquito vectors and avian reservoirs. Experiments modeling the entirety of the natural avian-mosquito-mammal transmission process of EEEV to determine the point(s) at which HS binding confers a replicative advantage and how these natural variants may influence this phenomenon are in progress.

ACKNOWLEDGMENTS

This work was supported by NIH grants 1R01AI095436 and 1R01AI083383 (to W.B.K.). J.H. acknowledges financial support by an International Outgoing Fellowship of the European Community program Support for Training and Career Development of Researchers (Marie Curie), under contract no. PIOF-GA-2009-235902.

We thank Matthew Dunn, Jenna Girardi, and Nicolas Garcia for their excellent technical assistance.

REFERENCES

1. **Griffin DE.** 2006. Alphaviruses, p 1023–1068. *In* Knipe DM (ed), Fields virology. Lippincott, Williams and Wilkins, Philadelphia, PA.
2. **Executive Office of Health and Human Services.** 2012. Arboviruses in Massachusetts— eastern equine encephalitis and West Nile virus. Executive Office of the Massachusetts Department of Health and Human Services, Boston, MA. http://www.mass.gov/dph/wnv.
3. **Mitchell CJ, Niebylski ML, Smith GC, Karabatsos N, Martin D, Mutebi JP, Craig GB, Jr, Mahler MJ.** 1992. Isolation of eastern equine encephalitis virus from Aedes albopictus in Florida. Science **257:**526–527.
4. **Gardner CL, Ebel GD, Ryman KD, Klimstra WB.** 2011. Heparan sulfate binding by natural eastern equine encephalitis viruses promotes neurovirulence. Proc. Natl. Acad. Sci. U. S. A. **108:**16026–16031.
5. **Silverman MA, Misasi J, Smole S, Feldman HA, Cohen AB, Santagata S, McManus M, Ahmed AA.** 2013. Eastern equine encephalitis in children, Massachusetts and New Hampshire, USA, 1970-2010. Emerg. Infect. Dis. **19:**194–201.
6. **Kjellen L, Lindahl U.** 1991. Proteoglycans: structures and interactions. Annu. Rev. Biochem. **60:**443–475.
7. **Rostand KS, Esko JD.** 1997. Microbial adherence to and invasion through proteoglycans. Infect. Immun. **65:**1–8.
8. **Byrnes AP, Griffin DE.** 1998. Binding of Sindbis virus to cell surface heparan sulfate. J. Virol. **72:**7349–7356.
9. **Bernard KA, Klimstra WB, Johnston RE.** 2000. Mutations in the E2 glycoprotein of Venezuelan equine encephalitis virus confer heparan sulfate interaction, low morbidity, and rapid clearance from blood of mice. Virology **276:**93–103.
10. **Heil ML, Albee A, Strauss JH, Kuhn RJ.** 2001. An amino acid substitution in the coding region of the E2 glycoprotein adapts Ross River virus to utilize heparan sulfate as an attachment moiety. J. Virol. **75:**6303–6309.
11. **Neff S, Sa-Carvalho D, Rieder E, Mason PW, Blystone SD, Brown EJ, Baxt B.** 1998. Foot-and-mouth disease virus virulent for cattle utilizes the integrin $\alpha_v\beta_3$ as its receptor. J. Virol. **72:**3587–3594.
12. **Lee E, Lobigs M.** 2008. E protein domain III determinants of yellow fever virus 17D vaccine strain enhance binding to glycosaminoglycans, impede virus spread, and attenuate virulence. J. Virol. **82:**6024–6033.
13. **Klimstra WB, Ryman KD, Johnston RE.** 1998. Adaptation of Sindbis virus to BHK cells selects for use of heparan sulfate as an attachment receptor. J. Virol. **72:**7357–7366.
14. **Smit JM, Waarts BL, Kimata K, Klimstra WB, Bittman R, Wilschut J.** 2002. Adaptation of alphaviruses to heparan sulfate: interaction of Sindbis and Semliki forest viruses with liposomes containing lipid-conjugated heparin. J. Virol. **76:**10128–10137.
15. **Brault AC, Powers AM, Chavez CL, Lopez RN, Cachon MF, Gutierrez LF, Kang W, Tesh RB, Shope RE, Weaver SC.** 1999. Genetic and antigenic diversity among eastern equine encephalitis viruses from North, Central, and South America. Am. J. Trop. Med. Hyg. **61:**579–586.
16. **Young DS, Kramer LD, Maffei JG, Dusek RJ, Backenson PB, Mores CN, Bernard KA, Ebel GD.** 2008. Molecular epidemiology of eastern equine encephalitis virus, New York. Emerg. Infect. Dis. **14:**454–460.
17. **Aguilar PV, Paessler S, Carrara AS, Baron S, Poast J, Wang E, Moncayo AC, Anishchenko M, Watts D, Tesh RB, Weaver SC.** 2005. Variation in interferon sensitivity and induction among strains of eastern equine encephalitis virus. J. Virol. **79:**11300–11310.
18. **Voss JE, Vaney MC, Duquerroy S, Vonrhein C, Girard-Blanc C, Cru-**

blet E, Thompson A, Bricogne G, Rey FA. 2010. Glycoprotein organization of Chikungunya virus particles revealed by X-ray crystallography. Nature **468:**709–712.
19. **Yin J, Gardner CL, Burke CW, Ryman KD, Klimstra WB.** 2009. Similarities and differences in antagonism of neuron alpha/beta interferon responses by Venezuelan equine encephalitis and Sindbis alphaviruses. J. Virol. **83:**10036–10047.
20. **Gardner CL, Burke CW, Tesfay MZ, Glass PJ, Klimstra WB, Ryman KD.** 2008. Eastern and Venezuelan equine encephalitis viruses differ in their ability to infect dendritic cells and macrophages: impact of altered cell tropism on pathogenesis. J. Virol. **82:**10634–10646.
21. **Klimstra WB, Ryman KD, Bernard KA, Nguyen KB, Biron CA, Johnston RE.** 1999. Infection of neonatal mice with Sindbis virus results in a systemic inflammatory response syndrome. J. Virol. **73:**10387–10398.
22. **Sali A, Blundell TL.** 1993. Comparative protein modelling by satisfaction of spatial restraints. J. Mol. Biol. **234:**779–815.
23. **Wang J, Wolf RM, Caldwell JW, Kollman PA, Case DA.** 2004. Development and testing of a general amber force field. J. Comput. Chem. **25:**1157–1174.
24. **Dolinsky TJ, Czodrowski P, Li H, Nielsen JE, Jensen JH, Klebe G, Baker NA.** 2007. PDB2PQR: expanding and upgrading automated preparation of biomolecular structures for molecular simulations. Nucleic Acids Res. **35:**W522–W525.
25. **Baker NA, Sept D, Joseph S, Holst MJ, McCammon JA.** 2001. Electrostatics of nanosystems: application to microtubules and the ribosome. Proc. Natl. Acad. Sci. U. S. A. **98:**10037–10041.
26. **Klimstra WB, Heidner HW, Johnston RE.** 1999. The furin protease cleavage recognition sequence of Sindbis virus PE2 can mediate virion attachment to cell surface heparan sulfate. J. Virol. **73:**6299–6306.
27. **Ryman KD, Gardner CL, Burke CW, Meier KC, Thompson JM, Klimstra WB.** 2007. Heparan sulfate binding can contribute to the neurovirulence of neuroadapted and nonneuroadapted Sindbis viruses. J. Virol. **81:**3563–3573.
28. **Tripathi CK, Banga J, Mishra V.** 2012. Microbial heparin/heparan sulphate lyases: potential and applications. Appl. Microbiol. Biotechnol. **94:**307–321.
29. **Desai UR, Wang HM, Linhardt RJ.** 1993. Specificity studies on the heparin lyases from Flavobacterium heparinum. Biochemistry **32:**8140–8145.
30. **Desai UR, Wang HM, Linhardt RJ.** 1993. Substrate specificity of the heparin lyases from Flavobacterium heparinum. Arch. Biochem. Biophys. **306:**461–468.
31. **Thompson SM, Fernig DG, Jesudason EC, Losty PD, van de Westerlo EM, van Kuppevelt TH, Turnbull JE.** 2009. Heparan sulfate phage display antibodies identify distinct epitopes with complex binding characteristics: insights into protein binding specificities. J. Biol. Chem. **284:**35621–35631.
32. **Mosier PD, Krishnasamy C, Kellogg GE, Desai UR.** 2012. On the specificity of heparin/heparan sulfate binding to proteins. Anion-binding sites on antithrombin and thrombin are fundamentally different. PLoS One **7:**e48632. doi:10.1371/journal.pone.0048632.
33. **Uniewicz KA, Ori A, Rudd TR, Guerrini M, Wilkinson MC, Fernig DG, Yates EA.** 2012. Following protein-glycosaminoglycan polysaccharide interactions with differential scanning fluorimetry. Methods Mol. Biol. **836:**171–182.
34. **Zhang W, Heil M, Kuhn RJ, Baker TS.** 2005. Heparin binding sites on Ross River virus revealed by electron cryo-microscopy. Virology **332:**511–518.
35. **Spear PG.** 2004. Herpes simplex virus: receptors and ligands for cell entry. Cell Microbiol. **6:**401–410.
36. **Griffin DE.** 1976. Role of the immune response in age-dependent resistance of mice to encephalitis due to Sindbis virus. J. Infect. Dis. **133:**456–464.
37. **Torrent M, Nogues MV, Andreu D, Boix E.** 2012. The "CPC clip motif": a conserved structural signature for heparin-binding proteins. PLoS One **7:**e42692. doi:10.1371/journal.pone.0042692.
38. **Meyer WJ, Johnston RE.** 1993. Structural rearrangement of infecting Sindbis virions at the cell surface: mapping of newly accessible epitopes. J. Virol. **67:**5117–5125.
39. **Byrnes AP, Griffin DE.** 2000. Large-plaque mutants of Sindbis virus show reduced binding to heparan sulfate, heightened viremia, and slower clearance from the circulation. J. Virol. **74:**644–651.
40. **Armstrong PM, Andreadis TG.** 2010. Eastern equine encephalitis virus in mosquitoes and their role as bridge vectors. Emerg. Infect. Dis. **16:**1869–1874.
41. **Weaver SC, Winegar R, Manger ID, Forrester NL.** 2012. Alphaviruses: population genetics and determinants of emergence. Antiviral Res. **94:**242–257.
42. **Crans WJ, McNelly J, Schulze TL, Main A.** 1986. Isolation of eastern equine encephalitis virus from Aedes sollicitans during an epizootic in southern New Jersey. J. Am. Mosq. Control Assoc. **2:**68–72.